Comparative Analysis of Harmonic Control Techniques in a Photovoltaic Microgrid with Simulation-Based Prediction

JIMMY TOAZA[1], JORGE GAVILANES[2], ROBERTO SALAZAR-ACHIG[1],
DIEGO L. JIMÉNEZ[1], JAVIER CULQUI-TIPAN[3]
[1]Facultad de Ciencias de la Ingeniería y Aplicadas,
Universidad Técnica de Cotopaxi,
Latacunga,
ECUADOR

[2]Departamento de Ciencias Exactas,
Universidad de las Fuerzas Armadas ESPE,
Sangolquí,
ECUADOR

[3]Departamento de Eléctrica, Electrónica y Telecomunicaciones,
Universidad de las Fuerzas Armadas ESPE,
Sangolquí,
ECUADOR

Abstract: - This research presents a comparative analysis with stochastic validation of three control strategies for harmonic mitigation in a 120 V photovoltaic microgrid subject to variable climatic conditions. The conventional MPPT (Perturb and Observe) control, MPPT with a tuned double passive filter, and the Fuzzy Logic Controller (FLC) were compared. The results obtained from the MATLAB/Simulink simulation indicated that the conventional MPPT system does not comply with the IEEE 519-2014 standard, registering a voltage THD (Total harmonic distortion) of 13.19 % and a current THD of 22.81 %. With the incorporation of the passive filter, the voltage THD was reduced to 0.69% and the current THD to 0.03 % in steady state. Meanwhile, the FLC proved to be a robust and adaptable solution because it algorithmically mitigated harmonics with a THD within the regulatory limits (4.09 %) and a THDi of 4.41 %. Furthermore, it reduced the settling time to 0.028 s with an improvement in power transfer at a useful current of 59 A. Finally, the model prediction was validated with Monte Carlo simulations based on 672 records with irradiance and temperature input data and load harmonic measurements taken with a Fluke analyzer 435, obtaining a relative error of 5.00 %.

Key-Words: - Active Power Filter, Harmonic Control Techniques, Harmonic Mitigation, MATLAB Simulation, Photovoltaic Microgrid, Power Quality.

Received: May 23, 2026. Revised: July 26, 2026. Accepted: August 27, 2026. Published: November 25, 2026.

1 Introduction

The increasing global demand for electricity, coupled with the need to reduce greenhouse gas emissions, is driving the integration of non-conventional renewable energy sources into electrical systems. One such source is solar photovoltaics, which has established itself as a viable alternative due to its availability and ease of integration into distributed generation systems [1]. Currently, grid-connected photovoltaic microgrids are enabling greater penetration of renewable energy, thus contributing to a resilient and sustainable transition in electrical systems.

However, the increasing integration of grid-connected photovoltaic systems (PVs) presents challenges, particularly regarding power quality. This is because one of the main components is the power electronic converters used for energy conversion and adaptation, which generate harmonics that affect the performance of the electrical grid and connected equipment [2]. The presence of harmonics increases energy losses, causing heating in conductors and transformers, which reduces the lifespan of the equipment and leads to grid stability problems [3].

Currently, the power quality in photovoltaic systems is evaluated by Total Harmonic Distortion

(THD), which is an indicator that quantifies the magnitude of the harmonics present in the voltage and current signals. These must comply with the international standard IEEE 519, which establishes maximum permissible limits to guarantee the proper functioning of electrical systems and minimize the adverse effects of the distortion generated in the converters of the PVS [4].

As an alternative to improve the performance of PVS, several authors have incorporated passive filters to reduce harmonic distortion levels [5]. These solutions increase the cost of implementation, the size of the system, and the complexity of the design [6].

On the other hand, the use of computational intelligence techniques, such as fuzzy logic-based controllers, shows favorable results in photovoltaic applications, as they improve system stability and reduce THD levels compared to conventional MPPT algorithms [7]. Fuzzy logic offers advantages in environments characterized by stochastic scenarios inherent to photovoltaic generation, which are due to variations in irradiance and temperature [8].

Although significant progress has been made, most research focuses on reducing harmonic distortion or optimizing energy in isolation, without considering prediction scenarios that reproduce the variable operating conditions present in real photovoltaic microgrids [9].

In the field of photovoltaic systems, the application of Monte Carlo simulation for harmonic analysis is a highly useful tool for evaluating the consistency of implemented control strategies, such as those of conventional MPPT controllers, MPPT with passive filters, and fuzzy controllers. It also allows for the generation of multiple probabilistic operating scenarios to analyze the evolution of Total Harmonic Distortion (THD) caused by variations in irradiance and load. This enables the determination of performance and the estimation of expected behavior under real-world uncertainty conditions [10]. It should be noted that several studies conclude that probabilistic methods allow for the characterization of harmonic behavior in electrical systems with high penetration of distributed energy resources, providing information on regulatory non-compliance and the operational reliability achieved with the implemented control strategies [11].

Therefore, the present research proposes to compare the conventional MPPT controller, the MPPT with passive filter, and the fuzzy controller for harmonic mitigation, in addition to probabilistically predicting the behavior of the total harmonic distortion by Monte Carlo simulation. The DC–AC conversion stage and the inverter PID control were based on the methodology presented in [12]. Building on these configurations, this study compares the P&O, P&O with passive filter, and FLC strategies in terms of their harmonic response. Finally, the obtained results were validated through Monte Carlo simulation.

2 Methods

The study is based on the performance of three control strategies used in a grid-connected photovoltaic microgrid, simultaneously considering harmonic distortion level indicators that must comply with IEEE 519 standards. The research will be developed in the MATLAB/Simulink environment, allowing the reproduction of controlled operating conditions and probabilistic scenarios that represent the real behavior of grid-connected photovoltaic systems.

2.1 Photovoltaic Microgrid Architecture

Figure 1 shows the architecture of the photovoltaic microgrid simulated in MATLAB-Simulink with the fuzzy controller. The system includes a photovoltaic module connected to a converter, controlled by an MPPT algorithm that calculates the power and voltage derivatives. The controller generates a reference current to produce PWM signals that regulate the converter and the DC-to-AC inverter. This powers a load synchronized with the grid, thus achieving optimal integration.

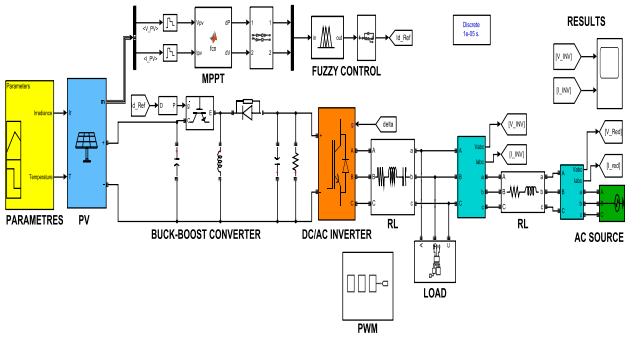

Fig. 1: Block diagram of the photovoltaic system simulated in MATLAB/Simulink
Source: created by the authors

Four monocrystalline solar panels were used, each with the electrical characteristics indicated in Table 1.

Table 1. Electrical characteristics of the photovoltaic modules

Parameter	Value
Short-circuit current (Isc)	13.95 A
Open-circuit voltage (Voc)	41.04 V
Nominal power (Pnom)	350 W
Type	Monocrystalline

Source: created by the authors

2.1.1 Mathematical Model of the Buck–Boost Converter

An averaged model operating in continuous conduction mode (CCM) was used to represent the dynamics of the Buck–Boost converter, considering the inductor current (i_L) and capacitor voltage (v_C) as state variables [13]. The duty cycle (D) was defined as the control variable, while (V_{PV}) represents the voltage supplied by the photovoltaic system. The inductor current dynamics are presented in Equation (1), whereas the capacitor voltage dynamics are given in Equation (2).

$$\frac{di_L}{dt} = \frac{D}{L}V_{PV} - \frac{1-D}{L}v_C \quad (1)$$

$$\frac{dv_C}{dt} = \frac{1-D}{C}i_L - \frac{v_C}{RC} \quad (2)$$

In the small-signal analysis around the operating point, the variables are expressed as $(i_L = I_{L0} + \widetilde{i_L})$, $(v_C = V_{C0} + \widetilde{v_C})$, $(D = D_0 + \tilde{d})$, and $(V_{PV} = V_{PV0} + \widetilde{v_{PV}})$, while the corresponding linearized model is presented in Equation (3).

$$\dot{\tilde{x}} = A_0\tilde{x} + B_d\tilde{d} + B_g\widetilde{v_{PV}} \quad (3)$$

The corresponding state-space matrix is presented in Equation (4).

$$A_0 = \begin{bmatrix} 0 & -\frac{1-D_0}{L} \\ \frac{1-D_0}{C} & -\frac{1}{RC} \end{bmatrix} \quad (4)$$

The characteristic polynomial used to analyze the stability of the converter is presented in Equation (5).

$$p(s) = s^2 + \frac{1}{RC}s + \frac{(1-D_0)^2}{LC} \quad (5)$$

For the SF analysis, real solar irradiance and temperature data were used; for this study, a data collection period of 7 days was considered, which adequately represents the climatic behavior of the month.

Subsequently, the recorded data were integrated into the photovoltaic microgrid model to be simulated in the MATLAB/Simulink software, with the purpose of obtaining a detailed analysis of the dynamic behavior of the system under real operating conditions.

Figure 2 and Figure 3 show, respectively, the evolution of ambient temperature and solar irradiance during one of the seven days of study. The incorporation of real data allowed the evaluation of the SF performance with the MPPT algorithm with a filter in addition to the fuzzy controller, obtaining the power quality curves produced under daily variations of irradiance and temperature, and providing a realistic operating simulation scenario.

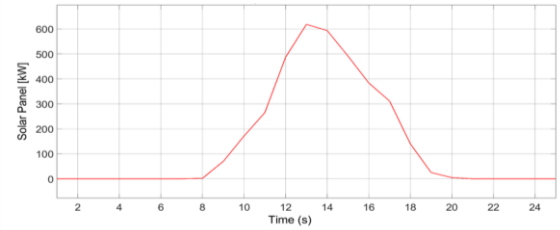

Fig. 2: Irradiance profile used in the simulation
Source: created by the authors

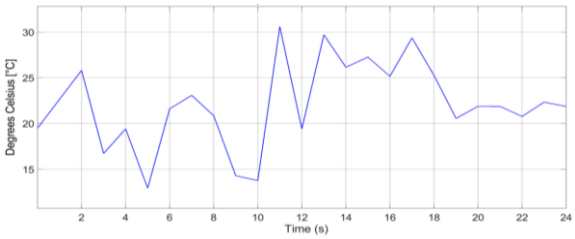

Fig. 3: Temperature profile used in the simulation
Source: created by the authors

2.2 Control Strategies Evaluated

Three control configurations will be implemented for the purpose of analyzing their influence on total harmonic distortion (THD) and their behavior under conditions of operational uncertainty.

2.2.1 Conventional MPPT

In this research, the Perturb and Observe (P&O) algorithm was implemented as a reference method for tracking the maximum power point (MPPT) of the SF, which contains a computationally low-cost algorithm.

The P&O method works by periodically disturbing the duty cycle of the DC-DC converter (Buck-Boost) in addition to the subsequent feedback of the effect produced on the output power of the photovoltaic panel [13]. At each sampling instant, the power is calculated using Equation (6), while the power and voltage variations are determined using Equations (7) and (8), respectively.

$$P(k) = V_{PV}(k)I_{PV}(k) \quad (6)$$

$$\Delta P = P(k) - P(k-1) \quad (7)$$

$$\Delta V = V_{PV}(k) - V_{PV}(k-1) \quad (8)$$

The P&O algorithm was programmed for simulation and applied to the Buck-Boost converter control. In this, a fixed disturbance step of 0.001 was used for the duty cycle, with the panel voltage and current signals being acquired at a sampling frequency of 10 kHz.

This method is the basis for comparison to evaluate the performance of the proposed fuzzy logic-based controller, thereby identifying improvements in harmonic reduction.

2.2.2 MPPT with Passive Filter

Subsequently, the maximum power point tracking (MPPT) algorithm based on the Perturb and Observe (P&O) method was implemented along with a passive filter on the AC side [14].

The DC-AC conversion stage was performed using a three-bridge inverter implemented with the Simulink Universal Bridge block. A PID controller regulated the inverter's switching, using the system frequency (60 Hz) as a reference [12]. To improve the power quality delivered to the grid, a double-tuned passive filter was incorporated at the inverter's output. The filter behavior and the impedance of each RLC branch are described by Equation (9).

$$Z_i(s) = R_i + sL_i + \frac{1}{sC_i}, \quad i = 1,2 \qquad (9)$$

The design parameters of this filter are shown in Table 2.

Table 2. Design parameters of the dual-tuned passive filter

Parameter	Magnitude
Inductance (L)	1.80 mH
Active power (Pa)	200 W
Quality factor (Qf)	15
Reactive power (Qc)	1 MVAR

Source: created by the authors

2.2.3 Fuzzy Controller

Figure 4 shows the input variables, which are the power (P) and voltage (V) of the photovoltaic panel. These variables were converted into fuzzy values using triangular membership functions, normalized in the interval [-1, 1], and divided into five linguistic sets, which are Large Negative (NG): [-1, -0.58], Medium Negative (NM): [-0.58, 0], Zero (Z): [-0.5, 0.5], Medium Positive (PM): [0, 0.58], Large Positive (PG): [0.58, 1].

This allows for a gradual representation of the degree of membership of each variable, making it possible to adequately obtain the uncertainty of the measurements under real operating conditions.

The fuzzy rule base was constructed using the Mamdani approach, in addition to if-then rules [15]. The controller output adjusts the duty cycle of the Buck-Boost converter, employing five sets of nomenclature (NG, NM, Z, PM, PG) with a small range [-0.01, 0.01]. This range allows for stable adjustments at the operating point of the SF, thus preventing large oscillations around the maximum power point.

The center of gravity (Centroid) method was applied, obtaining a fuzzy set with a numerical value output (crisp) [16]. This value is used as a reference signal to generate the PWM signal that controls the IGBT switch of the Buck-Boost converter, allowing dynamic adjustment of the operating point of the photovoltaic panel.

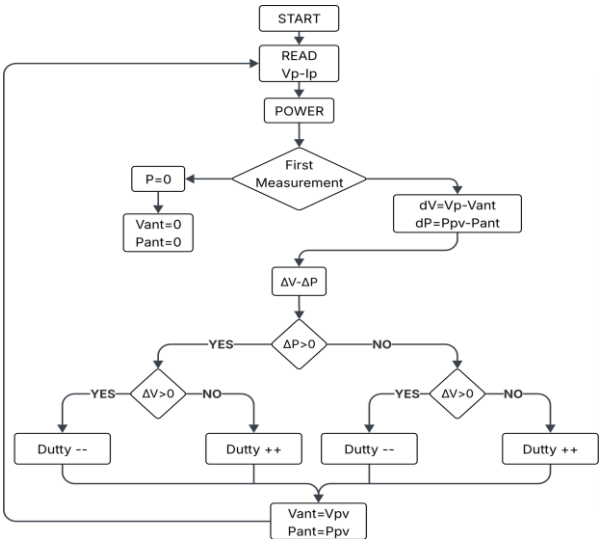

Fig. 4: Flowchart of the fuzzy logic control rules
Source: created by the authors

The rule evaluation was performed using the Mamdani inference method, in which the controller output corresponds to the duty-cycle adjustment (ΔD) of the Buck–Boost converter. The linguistic sets NG, NM, Z, PM, and PG were defined over the interval ($[-0.01, 0.01]$). The firing strength of each rule is determined using the minimum operator, as shown in Equation (10).

$$\alpha_i = \min\left[\mu_{A_i}(x_1), \mu_{B_i}(x_2)\right] \qquad (10)$$

The outputs generated by the rules are combined using the maximum operator, as shown in Equation (11).

$$\mu_{out}(z) = \max_i \left[\min\left(\alpha_i, \mu_{C_i}(z)\right)\right] \qquad (11)$$

2.3 Prediction of Total Harmonic Distortion using Monte Carlo Simulation

The Monte Carlo simulation method was implemented to predict the behavior of THD, based on the original time series obtained experimentally from the solar irradiance and temperature [17]. This generated multiple stochastic simulations to statistically analyze the variability of the SF in response to climatic variations. Furthermore, the statistical precision of the numerical method and the size of the simulations were quantified by calculating the standard error of the mean shown in Equation (12).

$$e = \frac{\sigma}{\sqrt{N}} \qquad (12)$$

Where:

e the standard error or required precision of the estimator.

σ the standard deviation of the simulated series. N corresponds to the total number of independent iterations or simulations performed.

This statistical criterion allows the predicted THD values to converge within an acceptable confidence range, meeting the harmonic distortion limits allowed by IEEE 519 regulations.

2.3.1 Harmonic Analysis and Predictive Evaluation

The harmonic distortion analysis is performed with the Fourier decomposition of the voltage and current signals captured at the point of coupling (PCC) [18]. Sampling was performed with the Fluke 435 power quality analyzer, and the Total Harmonic Distortion (THD) is calculated for each of the 672 records using Equation (13).

$$THD = \frac{\sqrt{\sum_{h=2}^{50} X_h^2}}{X_1} \times 100 \quad (13)$$

Where X_1 represents the effective (RMS) value of the 60 Hz frequency component. The harmonic analysis was performed from the second to the fiftieth harmonic order ($2 \leq h \leq 50$), in accordance with the range specified in IEEE 519- 2014 for harmonic distortion assessment. In addition to the overall THD, the individual harmonic components obtained through FFT analysis were also considered to identify the predominant harmonic orders.

3 Results

This section presents and analyzes the simulation results of the SF connected to the distributed electrical network to power an electronic load. Three scenarios were evaluated for the dynamic behavior of the system and the mitigation of harmonics.

3.1 Conventional MPPT Control without Active or Passive Filtering

The dynamic behavior of the system under conventional MPPT control (without a filtering stage) during transient operation is evaluated using time waveforms and analysis at the common coupling point (PCC). Figure 5 shows the instantaneous voltage and current signals recorded for this baseline scenario. It also shows that the phase current has a maximum operating amplitude of 31 A, while the line voltage stabilizes at a nominal value of 120 V. During the initial transient interval between t = 0 s and t = 0.045 s, the system experiences distortion and instability in these variables. This transient phenomenon is the dynamic response of the maximum power point tracking algorithm to the initial magnetization conditions of the inductive components and the load coupling. To quantify the steady-state harmonic distortion, the Fast Fourier Transform (FFT) algorithm was applied over a window corresponding to the first six operating cycles of the system phases. The results of the spectral analysis show Total Harmonic Distortion (THD) levels that exceed regulatory limits, with a voltage THD of 13.19 % and a current THD of 22.81 %.

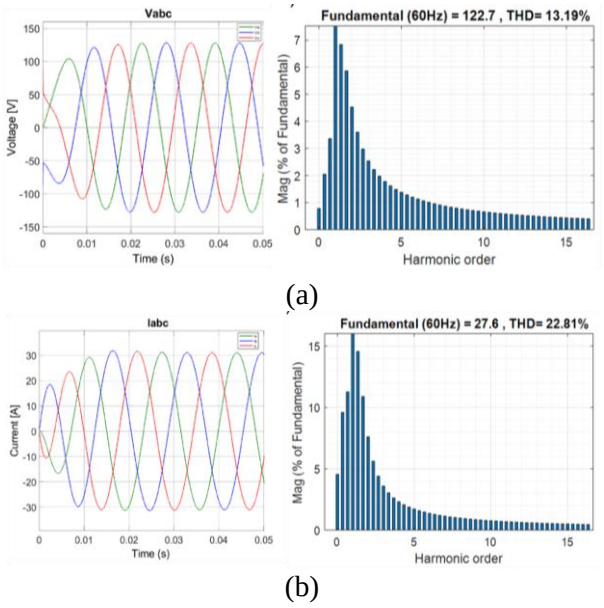

Fig. 5: MPPT control performance: a) Voltage signal and voltage THD level, b) Current signal and current THD level

Source: created by the authors

3.2 MPPT Control Coupled to a Tuned Passive Filter

The addition of the tuned passive filter in the inverter's output stage modified the equivalent impedance of the SF, mitigating the low-frequency harmonic components induced by the load. Figure 6 shows the instantaneous voltage and current waveforms for one of the three system phases under this configuration. The results obtained demonstrate a reduction in harmonic distortion compared to the base MPPT scenario. Spectral analysis using Fast Fourier Transform (FFT) quantified a voltage THD of 0.69 % and a current THD of 0.03 %. Comparing these values with the limits stipulated by the IEEE 519-2014 THD standard ≤8, it is identified that the values are within the regulatory compliance range, validating the effectiveness of the filter design. On the other hand, with respect to the temporal dynamic behavior, a slight transient disturbance was identified in the initial interval between t = 0 s and t = 0.01 s. This transient represents a 77.27 % reduction in the stabilization time compared to the scenario without a filter, which required 0.044 s. This is the result of the reactive

storage and dissipation capacity of the passive filter elements L and C, which absorb the inrush currents during load startup.

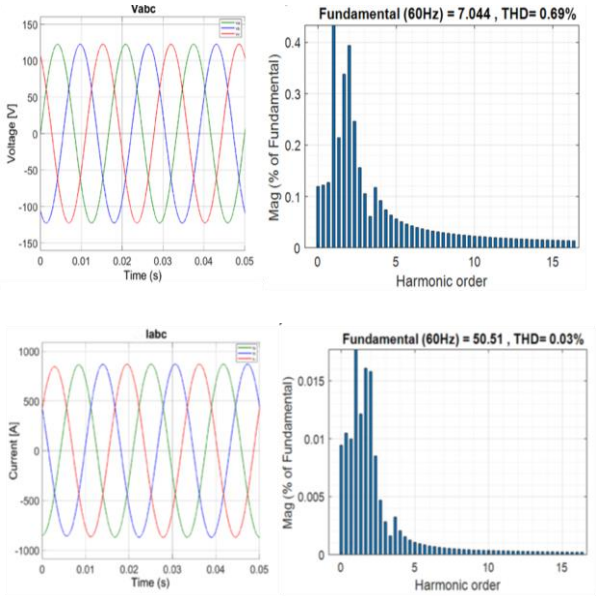

Fig. 6: MPPT control performance with passive filter: a) Voltage signal and voltage THD level with FPS, b) Current signal and current THD level with FPS
Source: created by the authors

3.3 System Interconnected by means of a Fuzzy Logic Controller

Finally, the performance of the photovoltaic system was evaluated by implementing MPPT control with the Fuzzy Logic Controller (FLC), which was designed to adapt the inverter switching to nonlinear load dynamics and intermittent weather. The resulting voltage and current waveforms are shown in Figure 7. The fuzzy controller values showed a stabilized voltage of 120 V and a current amplitude of up to 59 A. This increase in current magnitude (compared to 31 A in the conventional scenario) demonstrates the FLC's ability to optimize maximum power point tracking, thereby improving active power transfer to the load under variable coupling conditions. Power quality showed a voltage THD of 4.09 % and a current THD of 4.41 %. Comparing these values with the IEEE 519-2014 standard, it was found that the values are within the limits for low-voltage distribution systems. (Operating below 69 kV), the maximum tolerable THD value is 8 %, which is achieved without requiring external physical filtering elements. Furthermore, in the time domain, the initial transient distortion is 0.028 s in the simulation. This stabilization time with THD levels is longer than that obtained with the tuned passive filter, but the fuzzy controlled filter offers adaptability to changes. This demonstrates that while the passive filter has a fixed response and is susceptible to resonance phenomena when impedance changes occur in the network, the FLC provides a dynamic, adaptive harmonic attenuation response. The FLC is a robust alternative for environments characterized by nonlinear loads with variable generation profiles.

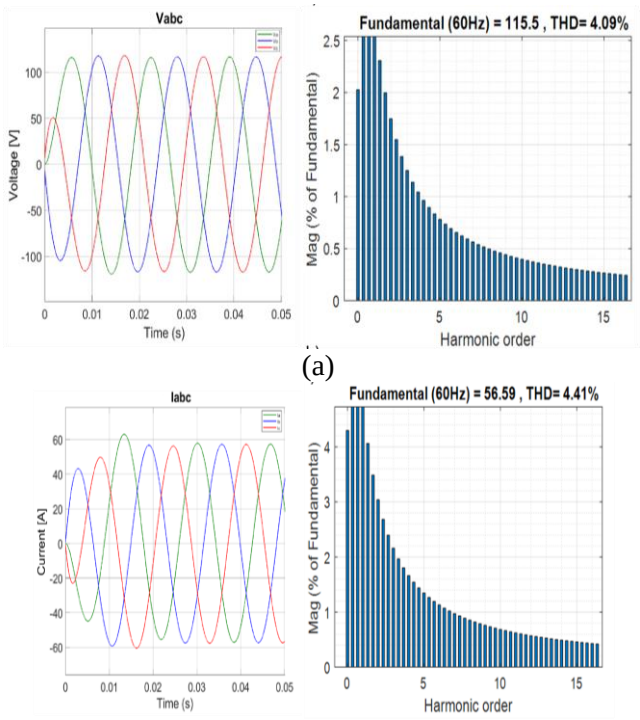

Fig. 7: FLC control performance: a) Voltage signal and voltage THD level, b) Current signal and current THD level
Source: created by the authors

Finally, the comparison identifies that the performance of the tuned Passive Filter represents the most efficient scenario in steady state, reducing THDv to a minimum of 0.69 % and THDi to 0.03 %. It also registers a shorter settling time of 0.010 s. However, despite this advantage, the literature indicates that passive filters introduce operational rigidity, meaning that a variation in the internal impedance of the nonlinear electronic load shifts the filter's resonance frequency, reducing its mitigation capacity in variable real-world environments. Meanwhile, the fuzzy logic control (FLC) without filtering hardware manages to mitigate harmonics, although its distortion indices THDv = 4.09 % and THDi = 4.41 % are close to the regulatory limit, remaining below the 8 % threshold of the IEEE 519-2014 standard for systems below 69 kV, with its response time of 0.028 s, which is 36.36 % faster than that of the conventional MPPT 0.044 s. The performance comparison of the evaluated strategies is presented in Table 3.

Table 3. Comparison of Total Harmonic Distortion (THD) and Settling Time for the Evaluated Control Techniques

Control Technique	THDv (%)	THDi (%)	Settling Time, (t_s) (s)
P&O	13.19	22.81	0.044
P&O + Passive Filter	0.69	0.03	0.010
FLC	4.09	4.41	0.028

Source: created by the authors

In conclusion, while the passive filter method offers maximum harmonic attenuation for fixed load conditions, the Fuzzy Logic Controller (FLC) is shown to be the most robust and technologically viable solution for modern photovoltaic microgrids, and the FLC is within the limits of the international regulatory standard, introducing variable flexibility which is essential to absorb stochastic disturbances of solar irradiance and changes in electronic loads.

3.4 Harmonic Prediction

For the prediction of the model with the stochastic climatic factors, the Monte Carlo method was applied for 7 days with the input variables that were parameterized from the changing profiles of solar irradiance and ambient temperature, running multiple simulations for the characterization of the variability of the SF. Statistical accuracy was validated by analyzing the standard error of the mean, ensuring that the results were within the operating limits admissible by IEEE 519-2014. Furthermore, the probabilistic predictive model was directly compared with experimental data, which consisted of 672 harmonic recordings captured in the field using a Fluke 435 power quality analyzer. The numerical results of the Monte Carlo iterations indicated a high degree of similarity with the experimental data from the photovoltaic inverter. The stochastic model accurately predicted a THD of 4.00 %, registering a relative percentage error of 5.00 % compared to the mean of the actual measurements. This relative error demonstrates that the probability distribution functions of the climatic variables and the mathematical model of the inverter adequately represent the actual physical phenomenon. Finally, the controlled dispersion shown by the simulated data confirmed that the probability of the system experiencing harmonic pollution events outside of power quality standards is minimal. The flow of the Monte Carlo scenario distribution is shown in Figure 8.

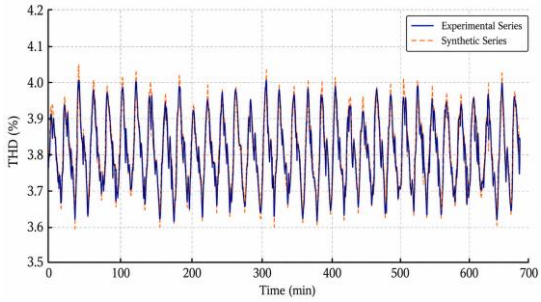

Fig. 8: Comparison of Experimental and Synthetic THD Series Obtained Using Monte Carlo Simulation
Source: created by the authors

Figure 9 shows the comparison between the experimental THD values and those obtained from the Monte Carlo simulation.

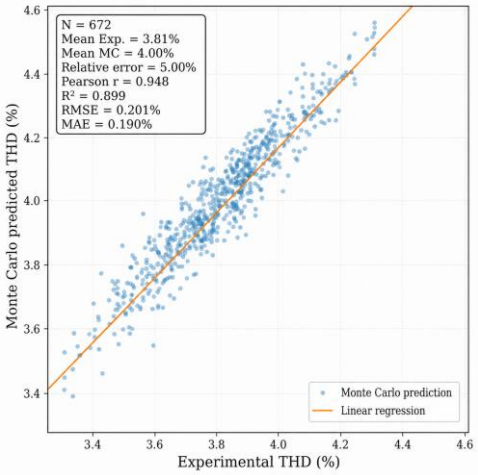

Fig. 9: Correlation between experimental and Monte Carlo predicted THD values
Source: created by the authors

Figure 9 shows the relationship between the experimental total harmonic distortion (THD) values and those calculated using the Monte Carlo simulation for a dataset of 672 observations. The experimental mean THD was 3.81 %, whereas the simulation yielded a mean value of 4.00 %, corresponding to a relative error of 5.00 %. The coefficient of determination (R^2 = 0.899) indicates good agreement between the simulated and experimental datasets. Furthermore, the RMSE of 0.201 % and MAE of 0.190 % show that the differences between the predicted and measured values remain within approximately 0.20 percentage points of THD, indicating close agreement between the simulation results and the experimental measurements. Overall, these results demonstrate that the Monte Carlo model adequately reproduces the variability observed in the experimental data, although the predicted THD values exhibit a slight tendency to overestimate the measured values.

4 Conclusion

The operation of the microgrid under a conventional MPPT control scheme (Perturb and Observe algorithm without filtering stages) does not meet power quality standards, having a total harmonic distortion of voltage THDv = 13.19 % and of current THDi = 22.81 %, the voltage distortion exceeds the 8 % limit established by IEEE Std 519-2014 [19], which indicated the need to incorporate active or passive attenuation technological solutions at the common coupling point (PCC).

The incorporation of the passive filter is an efficient alternative in steady-state for static load conditions, achieving purification of the waves that reached a THD of 0.69 % and a THDi of 0.03 %, with a lower transient stabilization time recorded t = 0.01 s, but in the comparative analysis it was determined that this has operational rigidity in the face of variations in dynamic environments. The Fuzzy Logic Controller (FLC) proved to be the solution that adapts to modern SF microgrids. It mitigated harmonics algorithmically without relying on large physical filters, achieving distortion indices in compliance with regulations, with a THDv = 4.09 % and THDi = 4.41 %. Furthermore, the controller improved active power transfer to the load, increasing the current to 59 A compared to 31 A for the MPPT system, with a 36.36 % reduction in stabilization time. Finally, the probabilistic Monte Carlo simulation, in which real climatic parameters were introduced and contrasted with 672 records measured with the Fluke 435 analyzer, validated the prediction of the system harmonics. The stochastic model indicated an average THD of 4.00% with a relative percentage error of 5.00 % compared to the field measurements, which indicates that the probability of operational failures or regulatory non-compliance is low in the developed FLC intelligent control.

Declaration of Generative AI and AI-assisted Technologies in the Writing Process

During the preparation of this work, the author(s) utilized artificial intelligence (AI) technologies solely for the purpose of linguistic refinement and grammatical correction. Following the application of these tools, the author(s) comprehensively reviewed, verified, and edited the resulting text. The author(s) maintain full accountability and responsibility for the accuracy, integrity, and final content of the publication.

References:

[1] G. Ferruzzi et al., Concentrating Solar Power: The State of the Art, Research Gaps and Future Perspectives, Energies, Vol. 16, No. 24, 2023, p. 8082. https://doi.org/10.3390/en16248082.

[2] J. Kaur and S. K. Bath, Harmonic distortion in power systems due to electronic control and renewable energy integration: a comprehensive review, Discover Electronics, Vol. 2, No. 1, 2025, p. 67. https://doi.org/10.1007/s44291-025-00111-9.

[3] Z. M. Ali, M. Ćalasan, F. Jurado, and S. H. E. Abdel Aleem, Complexities of Power Quality and Harmonic-Induced Overheating in Modern Power Grids Studies: Challenges and Solutions, IEEE Access, Vol. 12, 2024, pp. 151554- 151597. https://doi.org/10.1109/ACCESS.2024.3477729.

[4] M. Saleh Waseem Abbasi, S. A. A. Kazmi, M. Billah, A. Altamimi, Z. A. Khan, and M. Alghassab, Power quality optimization framework for three phase microgrids with grid tied solar PV and battery storage under nonlinear loads, Scientific Reports, Vol. 15, No. 1, 2025, p. 42568. https://doi.org/10.1038/s41598-025-18954-3.

[5] Subhajit Mukherjee, R. Mandal, and S. Chatterjee, Comparison of Harmonics Mitigation Techniques for Grid-Connected PV System and Introduction of a Concept of Hybrid Filter, Applied Solar Energy, Vol. 60, No. 1, 2024, pp. 138-148. https://doi.org/10.3103/S0003701X23601394.

[6] S. T. Y. Alfalahi, M. B. Mansor, A. Nouh, S. I. Abdrabba, and F. Mohamed, Sizing passive filters for mitigation of harmonics in a low voltage network containing solar PV units, Franklin Open, 2025, Art. 100220. https://doi.org/10.1016/j.fraope.2025.100220.

[7] T. M. de Lima and J. A. C. B. Oliveira, FPGA-Based Fuzzy Logic Controllers Applied to the MPPT of PV Panels—A Systematic Review, IEEE Transactions on Fuzzy Systems, Vol. 32, No. 8, 2024, pp. 4260–4269. https://doi.org/10.1109/TFUZZ.2024.3392846.

[8] D. Patel, S. Patel, P. Patel, and M. Shah, Solar radiation and solar energy estimation using ANN and Fuzzy logic concept: A comprehensive and systematic study,

Environmental Science and Pollution Research, Vol. 29, No. 22, 2022, pp. 32428-32442. https://doi.org/10.1007/s11356-022-19185-z.

[9] A. M. Abed, R. A. El-Sehiemy, B. Bentouati, and H. M. El-Arwash, Accurate Identification of Harmonic Distortion for Micro-Grids Using Artificial Intelligence-Based Predictive Models, IEEE Access, Vol. 12, 2024, pp. 83740-83763. https://doi.org/10.1109/ACCESS.2024.3400038.

[10] Y. Liu, K. Ding, J. Zhang, A. Sangwongwanich, and H. Wang, A Self-Data-Driven Method for Lifetime Prediction of PV Arrays Considering the Uncertainty and Volatility, IEEE Transactions on Power Electronics, Vol. 39, No. 3, 2024, pp. 3668-3682. https://doi.org/10.1109/TPEL.2023.3337713.

[11] A.-D. Olteanu, Ștefan Gheorghe, and G. Chicco, Artificial Intelligence-Driven Strategies for Management in Modern Utility Infrastructures: The Role of AI on Power Quality Management, in 2025 25th International Conference on Control Systems and Computer Science (CSCS), 2025, pp. 494-501. https://doi.org/10.1109/CSCS66924.2025.00079.

[12] M. Borja-Culqui, R. Salazar-Achig, D. L. Jiménez J., F. Vásquez, M. León, and J. Gavilanes, Analysis of harmonic mitigation in a photovoltaic energy microgrid for supply to an electronic load, in International Conference on Technological Innovation and AI Research (ICTIAIR 2025), 2025, pp. 64-71. https://doi.org/10.1049/icp.2025.1246.

[13] A. B. Djilali, A. Yahdou, H. Benbouhenni, A. Alhejji, D. Zellouma, and E. Bounadja, Enhanced perturb and observe control for addressing power loss under rapid load changes using a buck–boost converter, Energy Reports, Vol. 12, 2024, pp. 1503-1516. https://doi.org/10.1016/j.egyr.2024.07.032.

[14] R. Kahani, M. Jamil, and M. T. Iqbal, An Improved Perturb and Observed Maximum Power Point Tracking Algorithm for Photovoltaic Power Systems, Journal of Modern Power Systems and Clean Energy, Vol. 11, No. 4, 2023, pp. 1165–1175. https://doi.org/10.35833/MPCE.2022.000245.

[15] J. Sun and H. Xiang, Design of Type III Fuzzy Controller for Buck/Boost Converter, Journal of The Institution of Engineers (India): Series B, Vol. 105, No. 6, 2024, pp. 1611-1621. https://doi.org/10.1007/s40031-024-01055-6.

[16] M. Hashemi-Tabatabaei, M. Amiri, and M. Keshavarz-Ghorabaee, An Expected Value-Based Symmetric–Asymmetric Polygonal Fuzzy Z-MCDM Framework for Sustainable–Smart Supplier Evaluation, Information, Vol. 16, No. 3, 2025, p. 187. https://doi.org/10.3390/info16030187.

[17] K. Cajilema, R. Salazar-Achig, and D. L. Jiménez J., Analysis of the impact of solar radiation and temperature variations on grid-connected photovoltaic power generation, IOP Conference Series: Earth and Environmental Science, Vol. 1434, 2024, Art. 012012. https://doi.org/10.1088/1755-1315/1434/1/012012.

[18] S. Liao, Y. Tian, T. Gu, Z. Wang, L. Shang, and F. Liu, Analysis of Harmonic Characteristics in Distribution Network with Distributed PV, in 2024 IEEE 19th Conference on Industrial Electronics and Applications (ICIEA), 2024, pp. 1-5. https://doi.org/10.1109/ICIEA61579.2024.10664762.

[19] IEEE Standards Association, IEEE Recommended Practice and Requirements for Harmonic Control in Electric Power Systems, IEEE Std 519-2014, 2014. 10.1109/IEEESTD.2014.6826459

Contribution of Individual Authors to the Creation of a Scientific Article (Ghostwriting Policy)

The authors equally contributed to the present research, at all stages from the formulation of the problem to the final findings and solution.

Sources of Funding for Research Presented in a Scientific Article or Scientific Article Itself

Thanks to the Universidad de las Fuerzas Armadas ESPE for paying for the publication.

Conflict of Interest

The authors have no conflicts of interest to declare.

Creative Commons Attribution License 4.0 (Attribution 4.0 International, CC BY 4.0)

This article is published under the terms of the Creative Commons Attribution License 4.0 https://creativecommons.org/licenses/by/4.0/deed.en_US